NeuroImage: Clinical 36 (2022) 103215

Contents lists available at ScienceDirect

NeuroImage: Clinical

journal homepage: www.elsevier.com/locate/ynicl

Fornix alterations induce the disruption of default mode network in patients with adamantinomatous craniopharyngiomas

Jie Kang [a,1], Lei Cao [a,1], Taoyang Yuan [e], Lu Jin [a], Yanjiao He [f], Xing Liu [f], Cuiping Zhang [e], Nan Chen [g], Guofo Ma [a], Ning Qiao [a], Bochao Zhang [a], Wentao Wu [a], Yuanyu Shi [b,c], Hua Gao [e], Chuzhong Li [e], Yazhuo Zhang [e], Zhentao Zuo [b,c,d,*], Songbai Gui [a,*]

[a] Department of Neurosurgery, Beijing Tiantan Hospital, Capital Medical University, Beijing, China
[b] State Key Laboratory of Brain and Cognitive Science, Institute of Biophysics, Chinese Academy of Sciences, Beijing, China
[c] University of Chinese Academy of Sciences, Beijing, China
[d] Hefei Comprehensive National Science Center, Institute of Artificial Intelligence, Hefei, China
[e] Beijing Neurosurgical Institute, Capital Medical University, Beijing, China
[f] Department of Neuropathology, Beijing Neurosurgical Institute, Beijing Tiantan Hospital, Capital Medical University, China National Clinical Research Center for Neurological Diseases (NCRC-ND), Brain Tumor Center, Beijing Institute for Brain Disorders, Beijing Key Brain Tumor Laboratory, Beijing, China
[g] Psychiatry Research Center, Beijing Huilongguan Hospital, Peking University Huilongguan Clinical Medical School, 100096 Beijing, China

ARTICLE INFO

Keywords:
Craniopharyngioma
Cognitive
Default-mode network
Fornix

ABSTRACT

Adamantinomatous craniopharyngioma (ACPs) are rare embryonic tumors and often involve the hypothalamus. The underlying neural substrate of the hypothalamic involvement (HI)-related cognitive decline in patients with ACP is still unclear. We aimed to combine the multi-modal neuroimaging and histological characteristics of the ACP to explore the potential neural substrate of the HI-related cognitive decline. 45 patients with primary ACPs (invasive, 23; noninvasive, 22) and 52 healthy control subjects (HCs) were admitted to the cross-sectional study. No significant difference in cognitive domains was observed between HCs and patients with noninvasive ACPs (NACP). Patients with invasive ACPs (IACP) showed significantly lower working memory performance (WM, $p = 0.002$) than patients with NACP. The WM decline was correlated with the disruption of the medial temporal lobe (MTL) subsystem in the default mode network (DMN) ($r = 0.45$, $p = 0.004$). The increased radial diffusivity of the fornix, indicating demyelinating process, was correlated with the disruption of the MTL subsystem ($r = -0.48$, $p = 0.002$). Our study demonstrated that the fornix alterations link DMN disruption to HI-related cognitive decline in patients with ACPs. ACPs that invade the hypothalamus can provide a natural disease model to investigate the potential neural substrate of HI-related cognitive decline.

1. Introduction

Emerging studies have recognized hypothalamic involvement (HI) as a contributor to the cognitive decline of neurodegenerative diseases, such as Huntington's disease, Parkinson's disease, and frontotemporal dementia (Ishii and Iadecola, 2015; Neudorfer et al., 2021; Reppermund et al., 2007). Although recent reviews have addressed selected features of neurodegenerative diseases attributable to HI, such as systemic metabolic deficits or sleep abnormalities (Vercruysse et al., 2018), an appraisal of how HI affects the cognitive function in light of recent advances in both hypothalamic physiology and diseases pathobiology is conspicuously missing from the recent studies. Very limited research existed on the potential neural substrates of HI-related cognitive decline because the hypothalamus locates deeply in the brain with small size but

* Corresponding authors at: Department of Neurosurgery, Beijing Tiantan Hospital, Capital Medical University, No.119 South 4th Ring West Road, Fengtai District, Beijing, China (S. Gui). State Key Laboratory of Brain and Cognitive Science, Institute of Biophysics, Chinese Academy of Sciences, No.15 Datun Road, Chaoyang District, Beijing, China (Z. Zuo).

E-mail addresses: kangjie0919@163.com (J. Kang), caolei_163@163.com (L. Cao), 18810419140@163.com (T. Yuan), jinglu1001@163.com (L. Jin), heyanjiaoyj@139.com (Y. He), 1584659696@126.com (X. Liu), grassgrenn@163.com (C. Zhang), chenn414@163.com (N. Chen), maguofo@163.com (G. Ma), qiaoning2018@yeah.net (N. Qiao), 15822210280@163.com (B. Zhang), wuwentao1996@yeah.net (W. Wu), yyshi@bsclab.ibp.ac.cn (Y. Shi), huagao_bj@163.com (H. Gao), lichuzhong@163.com (C. Li), zyz2004520@yeah.net (Y. Zhang), zuozt@ibp.ac.cn (Z. Zuo), guisongbai@ccmu.edu.cn (S. Gui).

[1] Co-first authorship.

https://doi.org/10.1016/j.nicl.2022.103215
Received 22 June 2022; Received in revised form 28 September 2022; Accepted 29 September 2022
Available online 30 September 2022

diverse functions (Billot et al., 2020).

Among the suprasellar brain tumors, adamantinomatous craniopharyngioma (ACP) is a clinically challenging tumor because of its aggressive behavior.(Apps et al., 2018) ACP might develop at any point along the pituitary-hypothalamus axis.(Muller, 2014) The aggressive behavior of ACP would directly damage the hypothalamus, and lead to cognitive decline.(Muller et al., 2019) Based on the histological characteristics at the boundary of ACP, the ACPs were classified into two types: invasive ACP (IACP), thick capsule-like tissue, and/or infiltrating finger-like structures could be found at the junction of ACP and surrounding brain tissue; non-invasive ACP (NACP), a relatively clear cleavage could be found between the tumor and surrounding brain tissue.(Giese et al., 2019; Kawamata et al., 2005) In other words, the IACP had a more aggressive effect on the hypothalamus than NACP.(Conklin et al., 2019; Kang et al., 2021) Recently, neuroimaging evidence suggests that the cognitive decline in patients with ACP is associated with the grey and white matter changes in the fronto-limbic brain areas, which are brains regions enrolled in the default mode network (DMN).(Buckner et al., 2008; Uh et al., 2021b) Despite the HI being known a risk factor for cognitive decline in patients with ACP, very limited information exists regarding the correlation among ACP aggressive behavior, cognitive performance and the functional brain network analysis, which was critically important to underly the neural substrate of HI-related cognitive decline.The DMN is an intrinsic functional brain network whose constituent regions are spontaneously coactive and independent of external stimuli.(Andrews-Hanna et al., 2014) Recent studies have indicated the disruption of the DMN was related to the cognitive decline in patients with neuropsychiatric disorders.(Andrews-Hanna, 2012; Andrews-Hanna et al., 2014) The DMN involves overly intensive self-reference, attention, and working memory (WM),(Fan et al., 2020) but few studies explore the association among the HI, DMN changes, and WM decline.

Multi-mode imaging, including resting-state functional magnetic resonance imaging (rs-fMRI), diffusion tensor imaging (DTI), and voxel-based morphometry (VBM), has been used to analyze the functional brain network connectivity in a wide range of disorders related to cognitive decline.(Dijkhuizen et al., 2012) Rs-fMRI provides insight into the disrupted functional connectivity among structures in the DMN that results in memory processing impairments.(Chiesa et al., 2019) Memory and executive dysfunction in patients with mild cognitive impairment are associated with fractional anisotropy (FA) and mean diffusivity (MD) abnormalities in the basal forebrain, which are indicators derived from DTI.(Brueggen et al., 2015) The fornix is the predominant outflow tract of the hippocampal formation (HF), which is included in the MTL-subsystem of the DMN, and it connects with the mammillary bodies of the hypothalamus. The fiber connections between fornix and HF can be tracked using DTI.

In the present study, we used the ACPs that invade the hypothalamus as a natural disease model to evaluate the effect of ACP invasive behavior on cognitive status and brain changes via multi-mode imaging. We integrated the clinical data, multi-modal imaging, and histological characteristics of the tumor to explore the potential neural substrates of the HI-related cognitive decline, which may provide valuable approaches to treat HI-related cognitive decline.

2. Methods

2.1. Participants

Forty-five patients with primary ACPs who underwent surgery in the Beijing Tiantan Hospital from June 2018 to December 2019, were included in this study. The inclusion criteria for the patient group were 18–60 years of age and histologically proven ACP. No patients received steroids at the time of MRI and all patients were right-handed. The exclusion criteria were as follows: a history of stroke, cerebral trauma, brain surgery or brain radiotherapy, other intracranial abnormalities (i.e., arachnoid cyst), an inability to complete the MRI examinations, or preprocessing issues (i.e., head motion). The histological results of these patients were reviewed by two neuropathologists (YJ.H. and X.L.) to confirm the diagnosis of tumor invasion based on histological characteristics reported by Kawamata T.(Kawamata et al., 2005).

The cognitive status of 52 healthy controls (HCs) with matched age, sex, and educational background was determined. The following eligibility criteria were used for the HCs: the absence of known neurologic or psychiatric disorders, normal or corrected-to-normal vision, and normal hearing ability.

This study was approved by the medical ethics committee of Beijing Tiantan Hospital (KY 2018–053-02). Written informed consent was obtained from the legal representatives of all the patients and all the healthy volunteers in accordance with the Declaration of Helsinki.

2.2. Cognitive status assessments

The systematic neurocognitive performance tests were performed before surgery. Following a systematic interview and a physical examination by an independent physician, the patients underwent systematic neurocognitive tests supervised by a neuropsychologist (C.N.). The neurocognitive tests, including evaluation of verbal comprehension (VC), perceptual reasoning (PR), WM, and processing speed (PS), were measured using the Chinese version of WAIS-IV (PEARSON & HEALTHMEN Corp.) through 10 subsets: block design, similarities, digit span, matrix reasoning, arithmetic, vocabulary, symbol search, visual puzzles, coding, and information.

2.3. Pretreatment quality of life (QoL)

The EORTC QLQ-C30 is a questionnaire used to assess the health-related QoL in cancer patients (for details, see Supplemental eAppendix 1).

2.4. MRI acquisition

The scanning session for each patient included high-resolution structural T1 MRI, rs-fMRI, and diffusion tensor imaging (DTI) using a 3.0-T Siemens Prismafit scanner (Siemens Healthnieers, Erlanger, Germany) at the Beijing MRI Center for Brain Research, Institute of Biophysics, Chinese Academy of Sciences, with a 64-channel head coil. The T1w images were obtained with a 3D sagittal magnetization prepared rapid acquisition gradient echo sequence (resolution of 0.8 mm isotropic voxels; field of view = 256 × 256 mm2; 224 slices; flip angle = 8°; TI/TR/TE = 1000/2400/2.22 ms; data matrix = 320 × 320; bandwidth = 220 Hz/px; iPAT = 2). DTI acquisition was aligned with the anterior commissure posterior commissure plane. Diffusion sensitizing gradients were applied along 46 noncollinear directions with b-value = 1000&2000 s/mm2 and 7 scans without diffusion weighted, a phase inverse acquisition without diffusion gradients (TR = 3500 ms, TE = 86 ms, matrix = 140 × 140, field of view = 210 × 210 mm2 and 72 slices with 2 mm without gap). The rs-fMR images were obtained with an echo-planar image sequence (72 slices; TE = 30 ms; TR = 710 ms; flip angle = 54°; bandwidth = 2358 Hz/px; data matrix = 106 × 106; multiband factor = 8; field of view = 212 × 212 mm2 with a resolution of 2.0 mm isotropic voxels). During a 7-min and 41-s functional scan, patients were required to relax, not think of anything and gaze at a fixation point in the central screen throughout the session. After the scan, each subject was asked if he/she remained awake during the whole procedure. No patients received steroids at the time of MRI. The exclusion criteria of fMRI analysis were as follows: a history of stroke, cerebral trauma, brain surgery or brain radiotherapy, other intracranial abnormalities, an inability to complete the MRI examinations, or preprocessing issues (i.e., head motion). All images were coded to ensure investigator blindness to participant identification and diagnosis.

2.5. Data processing

2.5.1. Rs-fMRI preprocessing

The rs-fMRI data preprocessing was conducted with Statistical Parametric Mapping (SPM12, https://www.fil.ion.ucl.ac.uk/spm) and the Data Processing Assistant for Brain Imaging (DPABI, http://rfmri.org/dpabi). Data from five subjects were excluded due to excessive head motion. The first ten volumes were removed to avoid initial signal instability. The preprocessing steps comprised head motion correction, slice timing correction, spatial normalization to the standard Montreal Neurological Institute (MNI) brain space (2 mm), and spatial smoothing (6 mm full width half maximum Gaussian kernel). To eliminate physiological high-frequency cardiac and respiratory noise and reduce low-frequency drift, a temporal bandpass (0.01–0.1 Hz) was performed. Linear trend removal within each time series was also carried out. We used friston − 24 motion model for regression, which included 6 motion parameters of the current volume and the preceding volume, plus each of these values squared. The head motion, global brain signal, white matter signal and cerebrospinal fluid (CSF) signal were regressed out from the time course of rs-fMRI. Head motion of subjects < 3 mm or a 3° rotation in any direction was deemed acceptable. Data from five subjects were excluded due to excessive head motion ($n = 40$).Forty patients were enrolled in the neuroimaging analysis (Fig. 1, IACP, $n = 20$; NACP, $n = 20$).

The DMN comprises three distinct subsystems: the dorsal medial prefrontal cortex (DMPFC) subsystem, the medial temporal lobe (MTL) subsystem, and the core subsystem.(Andrews-Hanna et al., 2010b) Functional connectivity strength (FCS) changes within the DMN, i.e., the intra-FCS and inter-FCS of the three distinct subsystems in the DMN, were analyzed.

Functional-connectivity MRI analysis was performed using DPABI toolkit to extract the time series for each ROI (spherical radius of 5 mm). Eleven ROIs in the DMN subsystem for FC analysis were selected based on published data by Andrews-Hanna et al.(Andrews-Hanna et al., 2010). (supplemental Table 3) For each subject, we first calculated a Pearson's correlation and the significance level (i.e., p-value) between all given ROIs. Then, we obtained an 11×11 symmetric correlation matrix and the corresponding p-value matrix for each subject. Correlation coefficients matrix were converted into z-values with the application of Fisher's r-to-z transformation. The intra-subsystem functional connectivity strength (FCS) was defined as the mean of all FCS between regions within the selected subsystem. The inter-subsystem FCS was defined as the mean of all the FCS between any two ROIs across two selected subsystems. To examine which pairs of brain regional FCS contributed to the alterations in the DMN, the correlation coefficients between any two ROIs in the DMN were also compared between IACP group and NACP group using two-sample t-tests with false discovery rate correction.

2.5.2. Structural T1-MRI processing

Analysis of the right and left hippocampal volumes analysis was performed on the structural T1-MRI images by using the Freesurfer software package (http://surfer.nmr.mgh.harvard.edu). All T1-weighted images were visually inspected for motion artifact and gray-white contrast. The single acquisition with less motion artifact from each scan session was used so as not to introduce noise from the

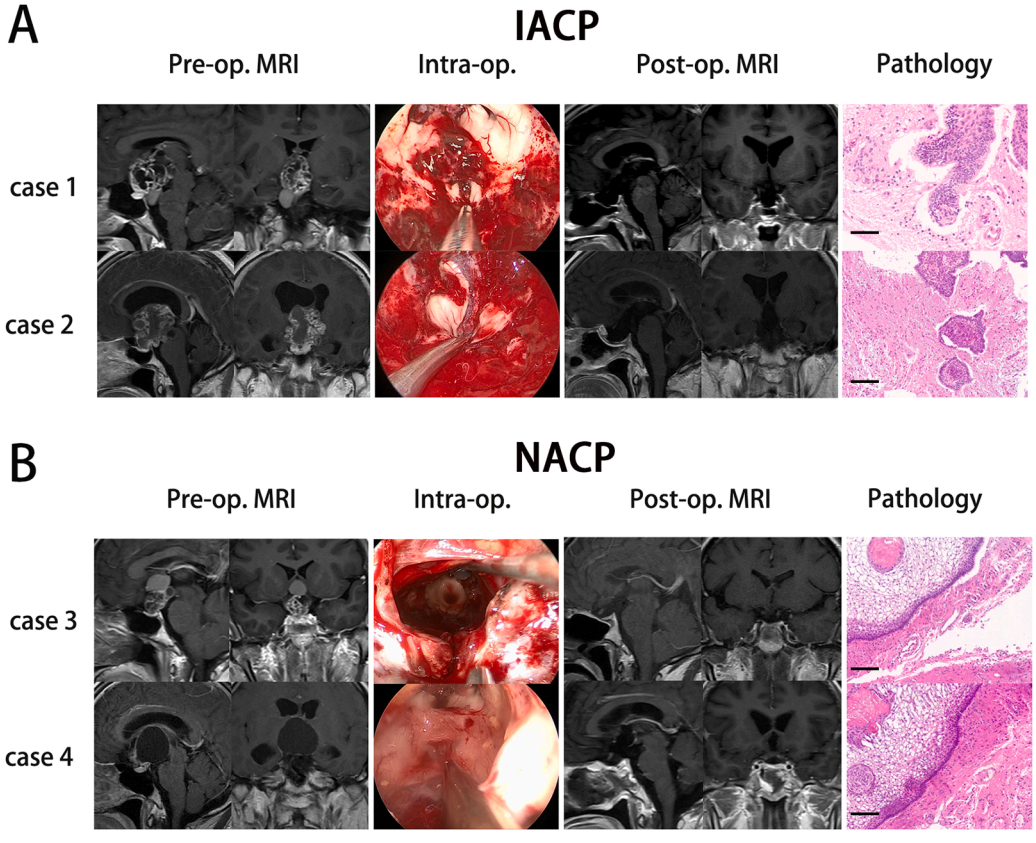

Fig. 1. The illustration of representative IACP and NACP cases. A: IACP: Case 1 and Case 2, pre-operative sagittal and coronal images demonstrated the suprasellar type craniopharyngioma. The tumors were totally removed through EEA. According to the pathologic image, the finger-like tumor structures invaded into the surrounding cerebral tissue. B: NACP: Case 3 and Case 4, pre-operative sagittal and coronal images demonstrated the suprasellar type craniopharyngioma. the tumor was totally removed through EEA. According to the pathological image, a relatively clear boundary could be found between the ACP and surrounding cerebral tissue. (scale bar: 300 μm).

additional volume. Cortical reconstruction and volumetric segmentation were performed. Right and left hippocampal volumes were calculated by voxel counting on binary hippocampal images segmented on T1-MRI data.

2.5.3. DTI processing

The fornix is the predominant outflow tract of the HF, which is included in the MTL-subsystem of the DMN, and it connects with the mammillary bodies of the hypothalamus. To investigate how the ACP affects the FC of the DMN, we speculated that the fornix, damaged by the aggressiveness of ACP, would show a correlation with alterations in the DMN. The FMRIB Software Library (FSL) version 6.0 was used for DTI processing (Oxford, UK; https://www.fmrib.ox.ac.uk/fsl). Raw 4D diffusion data were first corrected for Eddy current and motion distortions using twelve-parameter affine transformation. We used the Brain Extraction Tool to generate brain masks. A diffusion tensor model was fitted to every voxel in the brain to generate three eigenvectors and three eigenvalues. The eigenvalues were used to calculate FA, axial diffusivity (AD), MD, and radial diffusivity (RD). Each ROI was originally identified and manually drawn with high reliability using standardized guidelines based on T1w images. The fornix was determined by selecting fibers passing through seed and target ROI: seed ROI - mammillary body, target ROI - curs of the fornix.

2.5.4. Statistical analyses

Statistical analyses were performed using the SPSS software package (version 24, IBM Corp.). Descriptive analyses of demographic and clinical variables were conducted to characterize the group and compare participants to establish representativeness. Between groups, analyses were performed using a two-sample *t*-test with age and sex as covariates. To investigate the linear relationship between the variables, Pearson's product-moment correlation coefficient was computed, and the associated P value was assessed for significance. The P-value of < 0.05 was considered to be statistically significant.

3. Results

3.1. Demographic and clinical factors

The average age of 45 patients (male, n = 18; female, n = 27) was 39.3 ± 13.7 (male, 37.8 ± 15.4; female, 42.2 ± 12.6) years. The detailed demographic and clinical characteristics of patients and HCs (n = 52, 41.3 ± 13.7 years; male, n = 21, 39.9 ± 15.7 years; female, n = 31, 42.3 ± 12.3 years) are summarized in supplemental Tables 1 and 2. According to the histological characteristics at the boundary of ACP, the patients were classified into the invasive ACP (IACP, n = 23) group and the noninvasive ACP (NACP, n = 22) group. The representative cases of IACP and NACP were shown in Fig. 1.

3.2. IACP patients showed significantly lower cognitive performance

We compared the cognitive performance among the IACP group, the NACP group, and HCs. The IACP group showed significantly lower cognitive performance in WM (p = 0.008, p = 0.001), PS (p < 0.001, p < 0.001), VC (p = 0.002, p < 0.001), and PR (p = 0.021, p < 0.001) than the NACP group and HCs, respectively. No significant differences in the cognitive domains were observed between HCs and the NACP group (WM, p = 0.8; PS, p = 0.6; VC, p = 0.4; PR, p = 0.2). The cognitive status of all subjects was summarized in Table 1.

3.3. Relationship between cognitive status and QoL

Cognitive impairments in patients with ACP were found to significantly affect their QoL. Patients with IACP showed significantly lower QoL in physical function (p = 0.02), role function (p = 0.01), cognitive function (p = 0.006), social function (p = 0.02), and fatigue (p = 0.01).

Table 1
Cognitive Outcomes.

WAIS-IV	Control (n = 52)	ACP (n = 45)	IACP (n = 23)	NACP (n = 22)	P value
VCI (s.s)					
Mean ± SD (range)	107.1 ± 13.7 (78–131)	100.5 ± 14.8 (80–137)	96.3 ± 11.4 (76–117)	103.6 ± 16.5 (78–131)	* § ※
PRI (s.s)					
Mean ± SD (range)	106.2 ± 14.7 (76–140)	102.5 ± 18.0 (80–137)	98.0 ± 18.8 (61–122)	105.8 ± 17.0 (67–142)	* § ※
WMI (s.s)					
Mean ± SD (range)	103.1 ± 14.4 (68–131)	100.5 ± 15.1 (80–137)	95.1 ± 13.0 (68–119)	104.7 ± 15.6 (77–140)	* § ※
PSI (s.s)					
Mean ± SD (range)	102.4 ± 14.0 (76–125)	97.1 ± 20.3 (80–137)	93.0 ± 20.3 (45–125)	100.1 ± 20.3 (48–138)	* § ※

Notes: VCI: verbal comprehension index; PRI: perceptual reasoning; WMI: working memory index; PSI: processing speed index; *: HCs vs ACP, $p < 0.05$; §: HCs vs IACP, $p < 0.05$; ※: IACP vs NACP, $p < 0.05$.

The cognitive status tested by the systematic neurocognitive performance tests was significantly correlated with the QoL. The VC was significantly correlated with physical function (r = 0.38, p = 0.01), role function (r = 0.34, p = 0.02), cognitive function (r = 0.51, p < 0.001), and fatigue (r = 0.44, p = 0.002). The PR was significantly correlated with physical function (r = 0.32, p = 0.03), and cognitive function (r = 0.49, p < 0.001). The WM was significantly correlated with cognitive function (r = 0.35, p = 0.02). The PS was significantly correlated with social function (r = 0.53, p < 0.001), cognitive function (r = 0.75, p < 0.001) and fatigue (r = 0.65, p < 0.001).

3.4. The decreased FCS of the DMN, not alterations in hippocampal formation (HF) volumes, was associated with cognitive decline.

The ROIs of the three subsystems are described in Fig. 2A. According to the rs-fMRI results, the IACP group showed significantly lower FCS of the DMN (p = 0.003) than the NACP group (Fig. 2A). The FCS of the DMN was correlated with the PR (r = 0.37, p = 0.018) and WM (r = 0.60, p < 0.0001) in all patients (Fig. 2B). In the intra-subsystem analysis, the IACP group showed significantly decreased FCS of the MTL subsystem (p = 0.002) as compared to the NACP group (Fig. 2C). The intra-FCS of the MTL subsystem was correlated with the WM (r = 0.45, p = 0.004) in all patients (Fig. 2D). The rs-fMRI results demonstrated that the disruption of the MTL subsystem in the DMN was critically involved in the cognitive impairments in patients with ACP.

In the inter-regional FCS analysis in the DMN, two ROIs in the DMN concentrated in the HF showed significant differences in FCS as compared to other ROIs (Fig. 3A). The WM of patients was correlated with the FCs of PCC-Rsp (r = 0.51, p = 0.006), pIPL-Rsp (r = 0.48, p = 0.01), pIPL-PHC (r = 0.43, p = 0.02), and HF-Rsp (r = 0.42, p = 0.02) in the DMN (Fig. 3B and 3C). Between the IACP and NACP groups, no significant differences were observed in the left (3233.8 ± 455.8 vs 3549.9 ± 248.1 mm^3 (p = 0.25)) and right (3316.1 ± 546.7 vs 3417.3 ± 626.1 mm^3 (p = 0.59)) hippocampal volumes after adjustment for age, sex, and intracranial volume (Fig. 3D).

3.5. Alterations of the fornix were associated with the decreased FCS of the DMN.

The fornix, connected to the hypothalamus, is the predominant outflow tract of the HF, which is the major regional hub in the MTL subsystem. Thus, alterations in the fornix (Fig. 4A) were analyzed by DTI to further investigate the relationship between the invasiveness of ACP and MTL subsystem disruption in the DMN.

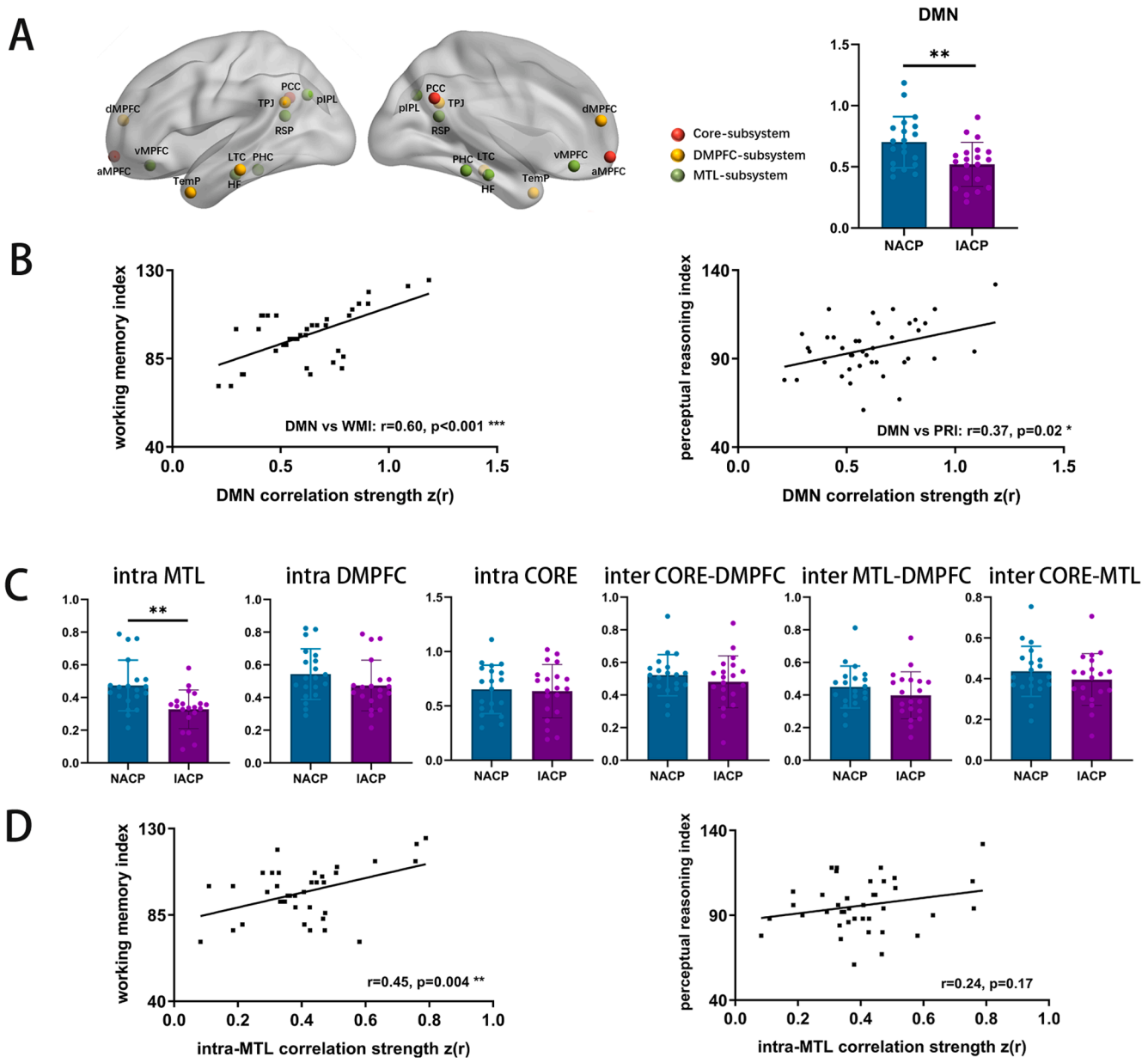

Fig. 2. Decreased FCS of the DMN and MTL subsystem were associated with the cognitive impairments. A: Illustrated the brain ROI regions of the DMN and its three subsystems, the core subsystem, the MTL subsystem and the DMPFC subsystem. The IACP group showed significantly lower FCS in the DMN than the NACP group (IACP, n = 20; NACP, n = 20). B: The FCS of the DMN was significantly correlated with the WM (r = 0.60, p < 0.001) and PR (r = 0.37, p = 0.02) in all patients. C: The IACP group showed significantly decreased FCS of the MTL subsystem in the intra-subsystem analysis (p < 0.01). D: The intra-FCS of the MTL subsystem was significantly correlated with the WM (r = 0.45, p = 0.004) in all patients. (*: p < 0.05, **: p < 0.01, ***: p < 0.001).

The fornix of the IACP group showed significantly decreased FA (p = 0.001), increased MD (p = 0.009), and radial diffusivity (RD, p = 0.003) values as compared to those of the NACP group (Fig. 4A). The increased RD of the fornix indicated the possibility of demyelinating changes. According to the DTI results, the increased RD of the fornix was correlated with the decreased FCS of the intra-MTL subsystem (r = -0.48, p = 0.002) (Fig. 4B).

4. Discussion

In this study, we integrated the clinical data, multi-modal imaging, and pathology characteristics of ACP to explore the neural substrates of HI-related cognitive decline.

4.1. Effect of ACP invasive behavior on cognitive status

ACP originated along with the pituitary–hypothalamic axis and often involved the hypothalamus, which was thought to be a risk factor for cognitive decline, including impairments of WM, PS, and attention. (Sterkenburg et al., 2015) ACPs that invade the hypothalamus can provide a natural disease model to investigate the neural substrate of HI-related cognitive decline. According to our results, patients with the IACP showed significantly lower preoperative cognitive performance in VC, PR, WM, and PS, which seriously affected their QoL, concentrating on physical function, role function, cognitive function, social function, and fatigue. It was in line with the post-operative findings of Muller et al. wherein ACP-related HI was correlated with cognitive deficits and poor QoL.(Mende et al., 2020) Therefore, it is essential to further explore the neural substrates of the impact of ACP invasive behavior on cognitive

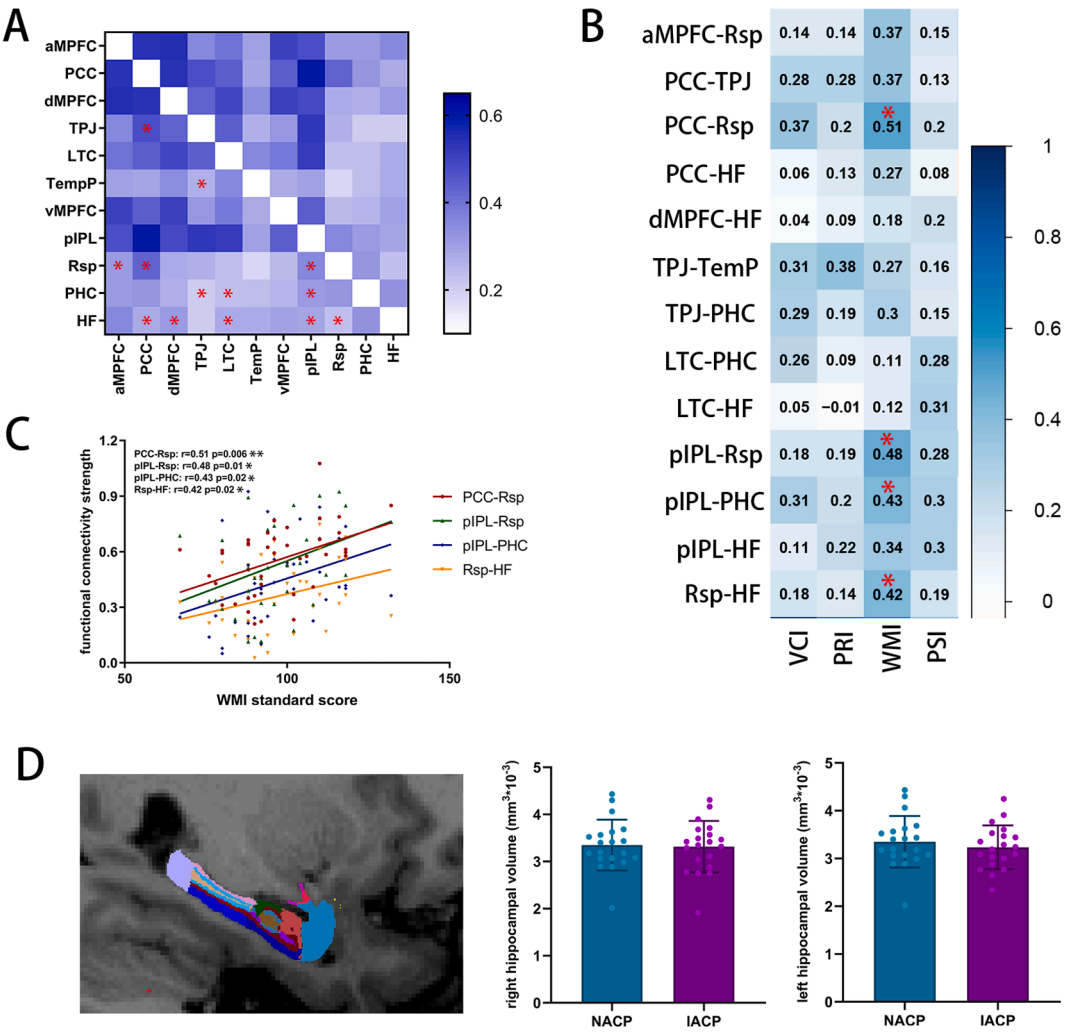

Fig. 3. HF connectivity disrupted, rather than HF volume alternation, was associated with cognitive impairments. A: The matrices showed that the coefficients between the ROIs in the DMN, and the significant differences between the IACP group (n = 20) and the NACP group (n = 20) were marked by red star ($p < 0.05$). The color bar indicates the correlation coefficients between regions. The significant differences concentrated on HF connections to other regions in the DMN. B: The matrices showed the coefficients between the significantly different inter-regional FCS of DMN and cognitive performance in patients (n = 40). The significant differences were marked by red star ($p < 0.05$). The color bar indicates the correlation coefficients. C: The significant different inter-regional FCS of DMN were significantly correlated with the WM (n = 40). D: MRI reconstruction of the hippocampus on native image. There were no significant differences in both right and left hippocampal volumes between the IACP group (n = 20) and the NACP group (n = 20). (*: $p < 0.05$, **: $p < 0.01$).

status.

4.2. *The potential neural substrate of HI-related cognitive impairments*

Previous studies have shown that the postoperative cognitive impairments were associated with white matter changes in the cingulum and prefrontal cortex in patients with CPs;(Fjalldal et al., 2018; Uh et al., 2021a) however, the association of the HI, brain changes and the cognitive decline was still unclear.

Multimodal neuroimaging can yield important insights into brain processes and structures, including: a comprehensive physiological view on brain processes and structures, quantification, generalization and normalization, and availability of biomarkers and has become a mainstay of basic and cognitive neuroscience in humans.{Uludag, 2014 #207} The functional brain network analysis is the consistent observation in human functional imaging and receives growing attention because of its association of neurocognitive performance.{Glover, 2011 #208} The brain networks contained the majority of highly connected regions and were described as the functional hubs. The hub regions are essential for optimal cognitive function because they ensure efficient integration of information between different brain regions.{Qi, 2018 #55} The DMN has a parallel level of complexity in the functional-anatomical organization to engage in the multiple-component processes of cognitive function.(Christoff et al., 2009; Grigg and Grady, 2010) The MTL-subsystem of DMN was associated with the WM in healthy subjects and patients with Alzheimer's disease.(Andrews-Hanna et al., 2010b; Qi et al., 2018) Our results also showed that the disruption of DMN was associated with the cognitive decline in patients with ACPs, and the lower FCS of the MTL subsystem was associated with the WM deficits ($r = 0.45$. $p = 0.004$). These results indicated that the disruption of DMN played a critical role in HI-related cognitive decline.

The HF plays a significant role in the MTL-subsystem, the resting MTL activity, and the MTL-cortical FC, which were related to individual differences in memory,(Wig et al., 2008) spontaneous episodic thoughts, (Andrews-Hanna et al., 2010a) and the consolidation of recent experiences.(Tambini et al., 2010) Our results revealed that the HF showed significantly different correlation coefficients as compared to other ROIs in DMN between the IACP group and the NACP group, and the FCS between the HF and brain regions in DMN was correlated with the cognitive performance. However, no significant difference in both left and right hippocampal volumes between the IACP and the NACP groups was found. Thus, we considered that the WM impairments in patients

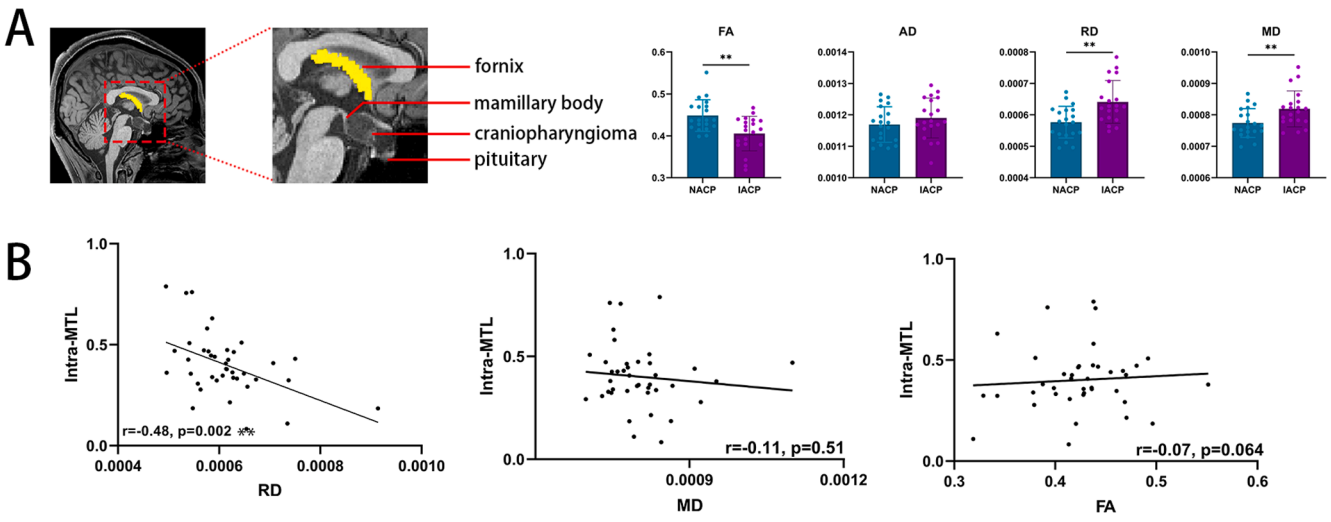

Fig. 4. Alterations of the fornix was associated with the decreased FCS of the DMN. A: Fornix region of interest (ROI) on a native image. Depictions of ROI placements on midsagittal slices to obtain the white matter voxels of the fornix body. The fornix of the IACP group (n = 20) showed significantly decreased FA and increased MD and RD as compared to that of the NACP group (n = 20). B: The increased RD of the fornix was correlated with the decreased FCs of the intra-MTL subsystem (n = 40, r = -0.48, p = 0.002).

with ACP were associated with the decreased FCS between the hippocampus and other brain regions in the DMN, rather than alterations in the hippocampus structure.

4.3. The fornix alterations link the HI to the disruption of the MTL subsystem in DMN

ACP is mostly located in the suprasellar region and involves the hypothalamus rather than the hippocampus directly. How does ACP affect the FCS of the MTL subsystem? Anatomically, the fornix is the predominant outflow tract that connects the hippocampus to the mammillary bodies of the hypothalamus. IACP often damages the surrounding hypothalamus tissue, including the mammillary bodies, which receive strong projections from the HF through the fornix.(Christiansen et al., 2016; Mielke et al., 2012) According to the DTI results in our study, the fornix of the IACP group showed significantly decreased FA (p = 0.001) and increased MD (p = 0.009) and RD (p = 0.003) as compared to those of the NACP group. The increased RD and MD of the white matter indicated demyelinating changes.(Janve et al., 2013; Wang et al., 2019) Our results demonstrated that the RD of the fornix increased in IACP, which indicated fornix demyelination was correlated with the decreased FCs of the intra-MTL subsystem (r = -0.48, p = 0.002).

Above all, our study showed that the ACP invasive behavior induced the fornix alterations. The fornix alterations were correlated with the decreased FCS of the MTL subsystem in the DMN. The disruption of the DMN was associated with cognitive decline in patients with ACP (Fig. 5). We demonstrated the correlations among the ACP invasive behavior, HI-related cognitive decline, the fornix alterations, and the DMN disruption, thus offering novel insights into the neural substrate of the HI-related cognitive decline.

The present study had several limitations. First, a comprehensive cognitive domain including an attention test and executive function test should be conducted in further studies. Second, a multicenter study based on a larger cohort with a long-term follow-up is needed in the future. Third, our research focused only on pretreatment subjects, which did not allow us to determine the specific changes in the fornix and DMN during the perioperative period. Fourth, our study had a small sample size. Considering these limitations, future work should involve a

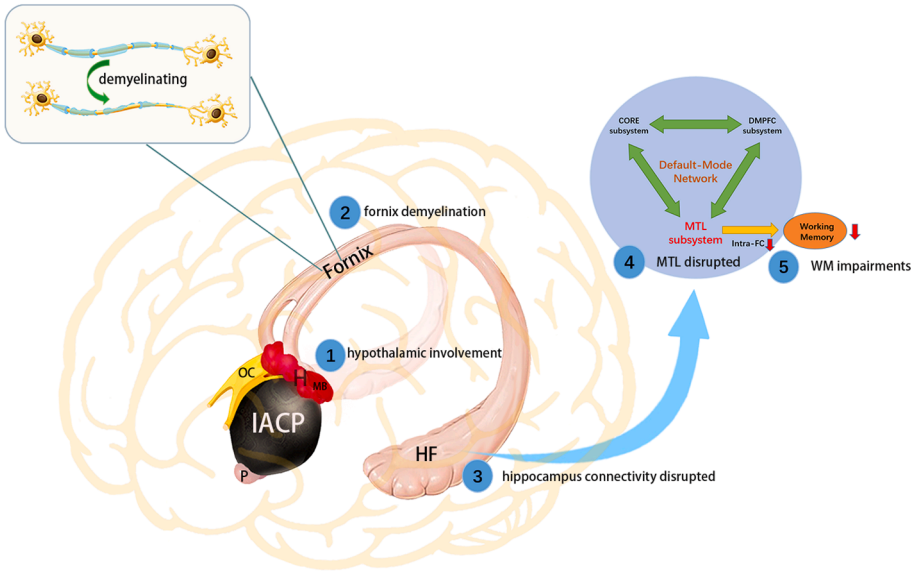

Fig. 5. Schematic summary of the neural substrate of cognitive decline in patients with ACP. ① IACPs invades MB of the hypothalamus and ② induces the alterations of the fornix. ③ The alterations of the fornix disrupts HF connectivity in MTL subsystem of DMN. ④The decreased intra-FCS of MTL-subsystem is significantly correlated with the WM impairments ⑤ in patients with ACP. P:pituitary; OC: optic chiasma; H: hypothalamus; MB: mammillary body; HF: hippocampal formation; MTL: medial temporal lobe; DMPFC: dorsal medial prefrontal cortex.

longitudinal study and include more participants in each group to enhance stability of the results. Furthermore, we will explore more reasonable ways to implement our research such as using the animal model to verify our results.

5. Conclusions

The invasive behavior of ACP induced the fornix alterations, which subsequently affected the FCS of the MTL subsystem in the DMN and resulted in WM deficits. Our study bridges the observations across the clinical data, multi-modal imaging, and histological characteristics of the ACP, thus offering novel insights into the neural substrate of the HI-related cognitive decline. It constitutes a promising step towards implementing personalized treatment for patients with HI-related cognitive decline.

6. Fundings

This study was supported by the Beijing Municipal Science & Technology Commission (Grant No. Z19110700660000), the National Natural Science Foundation of China (Grant No. 31730039), and Capital's Funds for Health Improvement and Research (Grant No. 2020-4-1077). The authors have no personal financial or institutional interest in any of the drugs, materials, or devices described in this article.

CRediT authorship contribution statement

Jie Kang: Conceptualization, Data curation, Formal analysis, Methodology, Writing – original draft, Writing – review & editing. **Lei Cao:** Conceptualization, Formal analysis, Methodology, Writing – original draft, Writing – review & editing. **Taoyang Yuan:** Conceptualization, Methodology, Writing – review & editing. **Lu Jin:** Data curation, Methodology, Writing – review & editing. **Yanjiao He:** Formal analysis, Methodology. **Xing Liu:** Data curation. **Cuiping Zhang:** Data curation. **Nan Chen:** Formal analysis, Methodology. **Guofo Ma:** Conceptualization, Data curation. **Ning Qiao:** Data curation. **Bochao Zhang:** Data curation. **Wentao Wu:** Data curation, Formal analysis. **Yuanyu Shi:** Data curation. **Hua Gao:** Formal analysis, Methodology. **Chuzhong Li:** Conceptualization. **Yazhuo Zhang:** Conceptualization. **Zhentao Zuo:** Conceptualization, Data curation, Formal analysis, Methodology, Writing – original draft, Writing – review & editing. **Songbai Gui:** Conceptualization, Data curation, Formal analysis, Methodology, Writing – original draft, Writing – review & editing.

Declaration of Competing Interest

The authors declare that they have no known competing financial interests or personal relationships that could have appeared to influence the work reported in this paper.

Data availability

Data will be made available on request.

Acknowledgments

We thank the PEARSON&HEALTHMEN Corp. for supervising and improving the confidence of the systematic neurocognitive performance tests and statistical analysis.

Appendix A. Supplementary data

Supplementary data to this article can be found online at https://doi.org/10.1016/j.nicl.2022.103215.

References

Andrews-Hanna, J.R., 2012. The brain's default network and its adaptive role in internal mentation. Neuroscientist 18, 251–270.
Andrews-Hanna, J.R., Reidler, J.S., Huang, C., Buckner, R.L., 2010a. Evidence for the default network's role in spontaneous cognition. J. Neurophysiol. 104, 322–335.
Andrews-Hanna, J.R., Reidler, J.S., Sepulcre, J., Poulin, R., Buckner, R.L., 2010b. Functional-Anatomic Fractionation of the Brain's Default Network. Neuron 65, 550–562.
Andrews-Hanna, J.R., Smallwood, J., Spreng, R.N., 2014. The default network and self-generated thought: component processes, dynamic control, and clinical relevance. Ann. N. Y. Acad. Sci. 1316, 29–52.
Apps, J.R., Carreno, G., Gonzalez-Meljem, J.M., Haston, S., Guiho, R., Cooper, J.E., Manshaei, S., Jani, N., Holsken, A., Pettorini, B., et al., 2018. Tumour compartment transcriptomics demonstrates the activation of inflammatory and odontogenic programmes in human adamantinomatous craniopharyngioma and identifies the MAPK/ERK pathway as a novel therapeutic target. Acta Neuropathol. 135, 757–777.
Billot, B., Bocchetta, M., Todd, E., Dalca, A.V., Rohrer, J.D., Iglesias, J.E., 2020. Automated segmentation of the hypothalamus and associated subunits in brain MRI. Neuroimage 223, 117287.
Brueggen, K., Dyrba, M., Barkhof, F., Hausner, L., Filippi, M., Nestor, P.J., Hauenstein, K., Kloppel, S., Grothe, M.J., Kasper, E., et al., 2015. Basal Forebrain and Hippocampus as Predictors of Conversion to Alzheimer's Disease in Patients with Mild Cognitive Impairment - A Multicenter DTI and Volumetry Study. J. Alzheimers Dis. 48, 197–204.
Buckner, R.L., Andrews-Hanna, J.R., Schacter, D.L., 2008. The brain's default network: anatomy, function, and relevance to disease. Ann. N. Y. Acad. Sci. 1124, 1–38.
Chiesa, P.A., Cavedo, E., Vergallo, A., Lista, S., Potier, M.C., Habert, M.O., Dubois, B., Thiebaut de Schotten, M., Hampel, H., group, I.N.-p.s,, et al., 2019. Differential default mode network trajectories in asymptomatic individuals at risk for Alzheimer's disease. Alzheimers Dement 15, 940–950.
Christiansen, K., Aggleton, J.P., Parker, G.D., O'Sullivan, M.J., Vann, S.D., Metzler-Baddeley, C., 2016. The status of the precommissural and postcommissural fornix in normal ageing and mild cognitive impairment: An MRI tractography study. Neuroimage 130, 35–47.
Christoff, K., Gordon, A.M., Smallwood, J., Smith, R., Schooler, J.W., 2009. Experience sampling during fMRI reveals default network and executive system contributions to mind wandering. Proc. Natl. Acad. Sci. 106, 8719–8724.
Conklin, H.M., Ness, K.K., Ashford, J.M., Scoggins, M.A., Ogg, R.J., Han, Y., Li, Y., Bradley, J.A., Boop, F.A., Merchant, T.E., 2019. Cognitive Performance, Aerobic Fitness, Motor Proficiency, and Brain Function Among Children Newly Diagnosed With Craniopharyngioma. J Int Neuropsychol Soc 25, 413–425.
Dijkhuizen, R.M., van der Marel, K., Otte, W.M., Hoff, E.I., van der Zijden, J.P., van der Toorn, A., van Meer, M.P., 2012. Functional MRI and diffusion tensor imaging of brain reorganization after experimental stroke. Transl Stroke Res 3, 36–43.
Fan, F., Tan, S., Huang, J., Chen, S., Fan, H., Wang, Z., Li, C.R., Tan, Y., 2020. Functional disconnection between subsystems of the default mode network in schizophrenia. Psychol. Med. 1–11.
Fjalldal, S., Follin, C., Svard, D., Rylander, L., Gabery, S., Petersen, A., van Westen, D., Sundgren, P.C., Bjorkman-Burtscher, I.M., Latt, J., et al., 2018. Microstructural white matter alterations and hippocampal volumes are associated with cognitive deficits in craniopharyngioma. Eur. J. Endocrinol. 178, 577–587.
Giese, H., Haenig, B., Haenig, A., Unterberg, A., Zweckberger, K., 2019. Neurological and neuropsychological outcome after resection of craniopharyngiomas. J. Neurosurg. 132, 1425–1434.
Grigg, O., Grady, C.L., 2010. The default network and processing of personally relevant information: converging evidence from task-related modulations and functional connectivity. Neuropsychologia 48, 3815–3823.
Ishii, M., Iadecola, C., 2015. Metabolic and Non-Cognitive Manifestations of Alzheimer's Disease: The Hypothalamus as Both Culprit and Target of Pathology. Cell Metab. 22, 761–776.
Janve, V.A., Zu, Z., Yao, S.Y., Li, K., Zhang, F.L., Wilson, K.J., Ou, X., Does, M.D., Subramaniam, S., Gochberg, D.F., 2013. The radial diffusivity and magnetization transfer pool size ratio are sensitive markers for demyelination in a rat model of type III multiple sclerosis (MS) lesions. Neuroimage 74, 298–305.
Kang, J., Cao, L., Yuan, T., Jin, L., Shi, Y., Ma, G., Qiao, N., Li, C., Zhang, Y., Zuo, Z., *et al.* (2021). Predicting the location of the preoptic and anterior hypothalamic region by visualizing the thermoregulatory center on fMRI in craniopharyngioma using cold and warm stimuli. *13*, 10087-10098.
Kawamata, T., Kubo, O., Hori, T., 2005. Histological findings at the boundary of craniopharyngiomas. Brain Tumor Pathol 22, 75–78.
Mende, K.C., Kellner, T., Petersenn, S., Honegger, J., Evangelista-Zamora, R., Droste, M., Stalla, G., Deutschbein, T., Wang, Y., Moskopp, D., et al., 2020. Clinical Situation, Therapy, and Follow-Up of Adult Craniopharyngioma. J. Clin. Endocrinol. Metab. 105.
Mielke, M.M., Okonkwo, O.C., Oishi, K., Mori, S., Tighe, S., Miller, M.I., Ceritoglu, C., Brown, T., Albert, M., Lyketsos, C.G., 2012. Fornix integrity and hippocampal volume predict memory decline and progression to Alzheimer's disease. Alzheimers Dement 8, 105–113.
Muller, H.L., 2014. Craniopharyngioma. Endocr. Rev. 35, 513–543.
Muller, H.L., Merchant, T.E., Warmuth-Metz, M., Martinez-Barbera, J.P., Puget, S., 2019. Craniopharyngioma. Nat Rev Dis Primers 5, 75.
Neudorfer, C., Elias, G.J.B., Jakobs, M., Boutet, A., Germann, J., Narang, K., Loh, A., Paff, M., Horn, A., Kucharczyk, W., et al., 2021. Mapping autonomic, mood and cognitive effects of hypothalamic region deep brain stimulation. Brain 144, 2837–2851.

Qi, H., Liu, H., Hu, H., He, H., Zhao, X., 2018. Primary Disruption of the Memory-Related Subsystems of the Default Mode Network in Alzheimer's Disease: Resting-State Functional Connectivity MRI Study. Front. Aging Neurosci. 10, 344.

Reppermund, S., Zihl, J., Lucae, S., Horstmann, S., Kloiber, S., Holsboer, F., Ising, M., 2007. Persistent cognitive impairment in depression: the role of psychopathology and altered hypothalamic-pituitary-adrenocortical (HPA) system regulation. Biol. Psychiatry 62, 400–406.

Sterkenburg, A.S., Hoffmann, A., Gebhardt, U., Warmuth-Metz, M., Daubenbuchel, A.M., Muller, H.L., 2015. Survival, hypothalamic obesity, and neuropsychological/psychosocial status after childhood-onset craniopharyngioma: newly reported long-term outcomes. Neuro Oncol 17, 1029–1038.

Tambini, A., Ketz, N., Davachi, L., 2010. Enhanced brain correlations during rest are related to memory for recent experiences. Neuron 65, 280–290.

Uh, J., Merchant, T.E., Conklin, H.M., Ismael, Y., Li, Y., Han, Y., Sabin, N.D., Babajani-Feremi, A., Indelicato, D.J., Hua, C.-H., 2021. Diffusion Tensor Imaging-Based Analysis of Baseline Neurocognitive Function and Posttreatment White Matter Changes in Pediatric Patients With Craniopharyngioma Treated With Surgery and Proton Therapy. Int. J. Radiat. Oncol.*Biol.*Phys. 109, 515–526.

Vercruysse, P., Vieau, D., Blum, D., Petersen, A., Dupuis, L., 2018. Hypothalamic Alterations in Neurodegenerative Diseases and Their Relation to Abnormal Energy Metabolism. Front. Mol. Neurosci. 11, 2.

Wang, C., Barnett, M.H., Yiannikas, C., Barton, J., Parratt, J., You, Y., Graham, S.L., and Klistorner, A. (2019). Lesion activity and chronic demyelination are the major determinants of brain atrophy in MS. Neurol. Neuroimmunol. Neuroinflamm *6*.

Wig, G.S., Grafton, S.T., Demos, K.E., Wolford, G.L., Petersen, S.E., Kelley, W.M., 2008. Medial temporal lobe BOLD activity at rest predicts individual differences in memory ability in healthy young adults. Proc. Natl. Acad. Sci. U.S.A. 105, 18555–18560.